Comparisons of chromophoric dissolved organic matter (cDOM) composition in small low and high Arctic catchments

Caroline Coch[1,2], Bennet Juhls[3], Scott F. Lamoureux[4], Melissa Lafrenière[4], Michael Fritz[1], Birgit Heim[1], and Hugues Lantuit[1,2]

[1] Alfred-Wegener-Institute Helmholtz Centre for Polar and Marine Research, Telegrafenberg A45, 14473 Potsdam, Germany
[2] University of Potsdam, Institute of Earth and Environmental Science, Karl-Liebknecht-Straße 24/25, 14476 Potsdam, Germany
[3] Freie Universität Berlin, Institute for Space Sciences, Department of Earth Sciences, 12165 Berlin, Germany.
[4] Queen's University, Department of Geography and Planning, Mackintosh-Corry Hall, Kingston, Ontario K7L 3N6, Canada

Correspondence to: Caroline Coch (coch.caroline@gmail.com)

Abstract. Climate change is an important control of carbon cycling, particularly in the Arctic. Permafrost degradation through deeper thaw and physical disturbances result in the release of carbon dioxide and methane to the atmosphere and to an increase in riverine dissolved organic matter (DOM) fluxes. Whereas riverine DOM fluxes of the large Arctic rivers are well assessed, knowledge is limited with regard to small catchments that cover more than 40 % of the Arctic drainage basin. Here, we use absorption measurements to characterize changes in DOM quantity and quality in a Low Arctic (Herschel Island, Yukon, Canada) and a High Arctic (Cape Bounty, Melville Island, Nunavut, Canada) setting with regard to geographical differences, impacts of permafrost degradation and rainfall events. We find that DOM quantity and quality is controlled by differences in vegetation cover and soil organic carbon content (SOCC). The Low Arctic site has higher SOCC and greater abundance of plant material resulting in higher chromophoric dissolved organic matter (cDOM) than in the High Arctic. Dissolved organic carbon (DOC) concentration and cDOM in surface waters at both sites show strong relationships similar to the one for the great Arctic rivers. We used the optical characteristics of DOM such as cDOM absorption, Specific UltraViolet Absorbance (SUVA), UltraViolet (UV) Slope and Slope Ratio (SR) for assessing quality changes downstream, at baseflow and stormflow conditions and in relation to permafrost disturbance. DOM in streams at both sites demonstrated optical signatures indicative of photodegradation downstream processes, even over short distances of 2000 m. Flow pathways and the connected hydrological residence time control DOM quality. Deeper flow pathways allow the export of permafrost-derived DOM (i.e. from deeper in the active layer), whereas shallow pathways with shorter residence times lead to the export of fresh surface and near-surface derived DOM. Compared to the large Arctic rivers, DOM quality exported from the small catchments studied here is much fresher and therefore prone to degradation. This has important implications for the carbon cycle, especially with regard to climate change. Optical properties of DOM will be a useful tool for understanding changes in DOM sources and quality at a pan-Arctic scale.

1 Introduction

Climate change has important impacts on carbon cycling, particularly in the Arctic. Approximately 1300 Gt of organic carbon are stored in permafrost soils in the northern hemisphere (Hugelius et al., 2014), which is 40 % more than currently circulating in the atmosphere. Thawing permafrost and deepening of the active layer leads to the mobilization of this carbon (Osterkamp, 2007; Woo et al., 2008), the release of carbon dioxide (CO_2) and methane (CH_4) to the atmosphere (Schaefer et al., 2014), and to an increase in riverine dissolved organic carbon (DOC) fluxes (Frey and Smith, 2005; Le Fouest et al., 2018). Associated with warming is also the development of surface (physical) disturbances such as active layer detachments or retrogressive thaw slumps (Lacelle et al., 2010; Lamoureux and Lafrenière, 2009; Lewkowicz, 2007; Ramage et al., 2018), and thermal perturbation of the subsurface (Lafrenière and Lamoureux, 2013). As these processes influence freshwater systems, they ultimately have impacts on the biological production and the biogeochemistry of the Arctic Ocean. The six largest arctic rivers (Mackenzie, Yukon, Ob, Yenisey, Lena, Kolyma) drain 53 % of the Arctic Ocean drainage basin (Holmes et al., 2012) and transport huge amounts of nutrients and dissolved organic matter (DOM) into the ocean. However, there are limited flux estimates and information on DOM quality available for the remaining 47 %, which are sourced by smaller watersheds. "Small" in this context refers to smaller than the large Arctic rivers as the actual size distribution remains unknown.

Terrigenous DOM is an important source of DOC originating from allochthonous (terrestrial such as soil and plants) and autochthonous (in situ production) sources (Aiken, 2014). It is modified by biotic and abiotic processes during its lateral transport to the ocean (Tank et al., 2018; Vonk et al., 2015a; Vonk et al., 2015b). Yet, little is known about the transformation of DOM along short distances in small catchments. The composition and the vulnerability to transformation of riverine DOM is influenced by several factors such as soil organic matter and vegetation, sorption processes in the mineral layers, and biodegradation and photodegradation processes (Cory et al., 2014; Mann et al., 2012; Vonk et al., 2015b; Ward and Cory, 2015; Ward et al., 2017). Chromophoric or colored dissolved organic matter (cDOM) is a fraction of DOM, which absorbs light in the ultraviolet and visible wavelengths (Green and Blough, 1994). Optical characteristics of cDOM such as absorption coefficients and spectral slopes can serve as proxies for DOM molecular weight and aromaticity, which in turn can help to characterize the lability of DOM (Helms et al., 2008; Neff et al., 2006; Spencer et al., 2009; Striegl et al., 2005; Weishaar et al., 2003).

Previous studies have focused on characterizing cDOM-DOC ratios for the large Arctic rivers and shelf areas, which exhibit a strong seasonality (Spencer et al., 2008; Stedmon et al., 2011; Walker et al., 2013). This was also shown by a global synthesis (Massicotte et al., 2017). A handful of studies have investigated cDOM-DOC relationships in smaller Arctic catchments: Dvornikov et al. (2018) examined cDOM characteristics in surface waters of the Yamal Peninsula and cDOM-DOC relationships were examined in studies of Subarctic catchments (Balcarczyk et al., 2009; Cory et al., 2015; Larouche et al., 2015; O'Donnell et al., 2014) and the High Arctic (Fouché et al., 2017; Wang et al., 2018). Optical parameters have also been used to assess the impact of permafrost disturbance on stream geochemistry in Alaska (Abbott et al., 2014; Larouche et al., 2015) and NWT Canada (Littlefair et al., 2017). As most studies focused on downstream reaches, knowledge on the spatial

variability across catchments is limited. To our knowledge, no study has examined this relationship in a Low Arctic setting or attempted to resolve geographic differences between the Low and High Arctic.

Here, we study cDOM and DOC in surface waters in the Low Arctic (Herschel Island, Yukon, Canada) and the High Arctic (Cape Bounty, Melville Island, Nunavut, Canada). The aim of this study is to (1) compare the variability and relation of DOC concentration and cDOM in High and Low Arctic surface water environments, and (2) to investigate changes in DOM composition along longitudinal stream profiles and with regard to permafrost disturbance and rainfall events. Climate change will substantially alter Arctic freshwater systems and carbon budgets. This study helps to understand and anticipate these changes.

2 Study Area

This study was carried out in two Arctic locations, Herschel Island in the Low Arctic and at the Cape Bounty Arctic Watershed Observatory, Melville Island in the High Arctic (Fig. 1a). Herschel Island (Yukon, Canada) is located at 69°35' N and 139°05' W in the Beaufort Sea off the Yukon coast. The island is composed of unconsolidated and fine-grained marine and glaciogenic sediments as it was formed by the Laurentide Ice Sheet (Mackay, 1959; Pollard, 1990). The island is situated in the zone of continuous permafrost with ground ice content between 30 and 60 % for the entire island. Physical permafrost degradation typically occurs in the form of retrogressive thaw slumps (Lantuit and Pollard, 2008) and active layer detachments (Coch et al., in review). Ramage et al. (2019) reported mean active layer depths of 52.2 ± 20.2 cm. Soil organic carbon content (SOCC) for valleys on the eastern side of Herschel Island was estimated to be 11.4 ± 3.7 kg m^2 at 0 - 30 cm depth and 26.4 ± 8.9 kg m^2 at 0 - 100 cm depth with a C:N ratio of 12.9 ± 2.2 in 0 - 100 cm depth (Ramage et al., 2019). The dominant vegetation type is lowland tundra (Myers-Smith et al., 2011; Smith et al., 1989) and can be classified into subzone E (CAVM, 2003), which corresponds to the Low Arctic. The mean annual air temperature and yearly precipitation between 1971 and 2000 at Komakuk Beach, the nearest long-term meteorological station ~40 km away from our study site, are -11 °C and 161.3 mm respectively. The mean July temperature is 7.8 °C and average precipitation is 27.3 mm (Environment and Climate Change Canada, 2018). Snowmelt is the largest hydrological event of the year occurring in May to early June. Summer baseflow from mid-June onwards is controlled by rainfall events (Coch et al., 2018). The active layer freezes up by mid-November (Burn, 2012). The studied catchments unofficially named Ice Creek West (1.4 km^2) and Ice Creek East (1.6 km^2) are adjacent to each other and merge into an alluvial fan before draining into the Beaufort Sea (Fig. 1b, Table 1). Both sampled ponds in Ice Creek West are below 1 ha large. There are degrading ice-wedge polygons present in the headwaters of Ice Creek West (Coch et al., in review). The Cape Bounty Arctic Watershed Observatory (CBAWO) is situated on the south coast of Melville Island (Nunavut, Canada) at 74° 55' N and 109° 35' W. The geology is characterized by Devonian sandstone and siltstone bedrock overlain by Quaternary marine and glacial sediments (Hodgson et al., 1984). The soils are categorized as cryosols with a thin organic horizon. The site is situated in the zone of continuous permafrost, and active layer depths typically range from 50 to 70 cm (Lafrenière et al., 2013). Permafrost degradation such as deep thaw and physical disturbances have altered hydrochemical fluxes of the rivers

(Lamoureux and Lafrenière, 2017). The vegetation cover is patchy with polar semi-desert, mesic tundra and wet sedge meadows (Edwards and Treitz, 2018), and falls into subzones B and C (CAVM, 2003). Soil organic carbon is estimated to be 3.0 kg m^2 in 0 - 30 cm depth, and 10.2 kg m^2 in 0 - 100 cm depth (Hugelius et al., 2013), with a C:N ratio of 10.0 in 0 - 100 cm depth (ADAPT, 2014). The nearest long-term meteorological station is located ~ 300 km away, at Mould Bay (NWT).

5 Between 1971 and 2000, the mean annual air temperature and precipitation were -17.5°C and 111 mm, respectively. The average July temperature is 4.0 °C, whereas mean precipitation is 13.5 mm. Snowmelt and nival flow typically start in early to mid-June with baseflow establishing around mid-July. Refreezing of the active layer starts mid- to late August (Lamoureux and Lafrenière, 2017; Lewis et al., 2012). Samples were taken downstream in Boundary River (152.5 km^2), its sub-catchment Robin Creek (14.8 km^2), and the neighboring watersheds West River (8.8 km^2) and East River (12.4 km^2) There is an active

10 retrogressive thaw slump in the Robin Creek watershed, and a number of recent (since 2007) active layer detachments and other disturbances in the West River watershed. The sampled lakes and ponds cover a range of sizes from below 1 ha in West River, to the larger West and East lakes (~120-140 ha).

3 Methods

3.1 Field methods and hydrochemistry

15 To explore downstream changes in DOM across regions, we used a transect approach in this study. Samples were taken along longitudinal stream profiles in catchments at Herschel Island and Cape Bounty (Fig. 1). Additionally, samples from standing water bodies (ponds and lakes) were collected. We further obtained discharge recordings and water samples from the outflow of both catchments at Herschel Island over the course of the summer as detailed below.

Field work on Herschel was carried out in July-August 2016. We measured discharge using a cutthroat flume equipped with a

20 U20 Onset Hobo level logger in Ice Creek West. Discharge data at 30 minute intervals is available from 15 May 2016 and at 5 minute intervals after 22 July 2016 (Coch et al., 2018; Coch et al., in review). In Ice Creek East, discharge was determined using the area velocity method in combination with a U20 Onset Hobo level logger (see Coch et al. in review for a detailed description). Data in Ice Creek East is available at 5 minute intervals after 25 July 2016. Weather data is available from the local Environment and Climate Change Canada Station, and from a station deployed in Ice Creek West during the summer.

25 Water samples were collected after triple rinsing the sampling bottle at the outflow of both streams between 20 July and 10 August. At the outflow of Ice Creek West, water samples were collected using an automatic water sampler (ISCO 3700) at a 12-hour interval between 25 July and 10 August and more frequently during rainfall events (between 1-3 hours). Prior to the automatic sampling, and also in Ice Creek East, water samples were taken manually once per day. We collected water samples (11 in Ice Creek West, 12 in Ice Creek East) along longitudinal profiles of the channels starting in the headwaters (~ 2000 m

30 distance from the outflow) and following the river downstream (Fig. 1). This was done 3 times in Ice Creek West (20, 25 and 30 July) and once in Ice Creek East (30 July). Samples of flowing waters are available from Ice Creek West (n=90), Ice Creek

East (n=32) and the alluvial fan (n=8). Standing water samples (n=4) were collected from 2 ponds in the Ice Creek West catchment.

The field work at Cape Bounty took place in August 2017. All water samples were collected manually after triple rinsing the sampling bottle. Similarly to the Herschel field work, we collected samples along longitudinal stream profiles. Robin Creek is
5   a subcatchment of Boundary River (Fig. 1), where stream samples were collected at six locations downstream of a retrogressive thaw slump. Three lakes were also sampled in the Boundary river catchment, and 2 samples from the main river channel. A total of 21 river samples and 9 samples from lakes and ponds are available from the West River catchment, some of which were collected after the rainfall event on 12 August 2017. In East River, 4 samples are available from the stream and 8 samples from standing water bodies.

10   Within 24 hours of sampling, electrical conductivity and pH were measured in the field lab. After collection, water samples were filtered through pre-rinsed 0.7 µm GF/F syringe filters and where then stored cool and dark for transport to the Alfred-Wegener-Institute, University of Hamburg and Geoscience Research Centre GFZ, Germany, where analysis for DOC and cDOM were carried out. Samples for DOC analyses were acidified with HCl (30 % suprapur) prior to the measurements. In 2016, DOC measurements were performed on a Shimadzu TOC-L analyzer with a TNM-L module (University of Hamburg),
15   whereas a Shimadzu TOC-VCPH analyzer was used in 2017 (AWI). The error for these measurements is below 10 %. Inorganic carbon (TIC) was sparged out using synthetic air prior to the measurement. As we had a shortage of HCl in the field in 2016, 82 of the samples were frozen and acidified upon return to Germany. After new acid was acquired later in the summer, sample duplicates (n=47) were processed directly in the field and also frozen. The frozen duplicate was thawed and acidified upon return to determine the effect of different sample treatment (Coch et al. 2018). There is a significant linear relationship
20   ($p < 0.05$, $n = 47$, $R^2 = 0.87$) between DOC concentrations of unfrozen and frozen sample duplicates. Samples that were frozen in the field, and subsequently thawed and acidified upon return to Germany showed lower DOC concentrations (by 13%) than samples that were acidified directly in the field and kept unfrozen. We corrected the frozen samples for this offset (Supplementary S1). In both years, deionized water used in the field was also analyzed as blank following the same procedure. The absorbance of cDOM was measured on a LAMBDA 950 UV/Vis Spectrophotometer (GFZ Potsdam) for the wavelength
25   from 200 to 800 every 1 nm (average of duplicates) using a 5cm cuvette and Milli-Q water as a reference to check for instrument drift. Some of the water samples showed fine particles precipitated in the sample bottle. They appeared in the form of small thin flakes, which partly remained in suspension or accumulated at the bottom of the flask. This precipitation occurred after the samples were filtered through 0.7 µm glass fiber filters, transported to the laboratory for storage of about 4 weeks. This was noted down in the lab, and absorbance spectra were not further analyzed for those samples as interference of the
30   spectral characteristics by the particles might have occurred. This was the case for 25 (out of 55) samples at Cape Bounty and for 8 samples (out of 134) at Herschel Island.

The Naperian spectral absorption coefficient of cDOM ($a_{cDOM}(\lambda)$) was calculated with

$$a_{CDOM}(\lambda)\ (m^{-1}) = \frac{2.303 * A_\lambda}{L}, \hspace{4cm} (1)$$

where A_λ is the absorbance and L the optical path length of the used cuvette in the spectrophotometer. The absorption was corrected for scatter using a baseline correction by subtracting $a_{cDOM}(700)$ (Hancke et al., 2014; Helms et al., 2008). At that wavelength, absorption by cDOM is assumed to be negligible (Mitchell et al, 2002). Spectral slopes of a_{cDOM} for wavelength ranges from 275 to 295nm (S275-295) and 350 to 400nm (S350-400) were calculated using Eq. (2) and a non-linear fit. These

5   slopes indicate photochemical or microbial alteration of DOM (Helms 2008). The ratio of both slopes (S275-295 : S350-400) defines the slope ratio (SR). The SUVA (mg L^{-1} m^{-1}) was calculated by dividing the decadal absorption (A_{254} / L) at 254 nm (m^{-1}) by DOC (mg l^{-1}). Both parameters have been related to the relative molecular weight and aromaticity of DOM (Helms et al., 2008; Weishaar et al., 2003).

$$a_{CDOM}(\lambda)(\lambda) = a_{CDOM}(\lambda_0) * e^{-S(\lambda - \lambda_0)}, \hspace{3cm} (2)$$

10   Where λ_0 is the absorption coefficient at reference wavelength and S is the spectral slope of $a_{CDOM}(\lambda)$ for the chosen wavelength range. To compare our data with different studies we converted absorption coefficient reported in various studies to $a_{cDOM}350$ using an interpolation method developed by Massicotte et al. (2017).

Throughout the manuscript all data is reported as mean ± standard deviation.

3.2 Statistical Analyses

15   We used RStudio (Version 1.0.153) to perform statistical tests (RStudio Team, 2016). Normality was tested using the Shapiro-Wilk normality test. To determine the difference in means of two populations, we applied the Welch's two sample t-test if the data was normally distributed with unequal variances. In the case of not normally distributed data, we used the Wilcoxon-Mann-Whitney test. To measure the relationship between two variables, we used the Pearson correlation coefficient for normally distributed data and the Spearman rank correlation if the data was not normally distributed.

20   **4 Results**

4.1 Meteorological conditions and general hydrochemistry

The mean annual air temperature on Herschel Island was -6.3 °C in 2016 with mean temperatures of 9.4 °C in July and 7.7 °C in August. During the monitoring period, rainfall events of 33.9 mm (19 July), 9.3 mm (30 July) and 12.7 mm (5 August) were recorded. CABWO had a mean annual air temperature of -15.3 °C in 2017, with mean air temperatures of 4.5 °C in July and

25   1.6 °C in August. During the monitoring period, two rainfall events of 0.2 mm (4 August) and 1.2 mm (8 August) occurred. Electrical conductivity (EC) and pH are significantly higher (p < 0.05) in surface waters on Herschel Island (1050 ± 370 µS cm^{-1} and 8.2 ± 0.2 µS cm^{-1}) than at Cape Bounty (137 ± 136 µS cm^{-1} and 7.2 ± 0.5 µS cm^{-1}). Whereas no difference was found for these parameters between standing and flowing water on Herschel Island, pH and EC were significantly higher in standing water at Cape Bounty than in flowing water (Table 2). Robin Creek showed highest EC values and the largest variability (145

30   ± 213 µS cm^{-1}) of the Cape Bounty rivers, whereas West River showed the overall lowest EC values (60 ± 17 µS cm^{-1}). On

Herschel Island, both adjacent rivers show EC and pH values in the same order of magnitude with a slight decrease at the alluvial fan outflows.

4.2 DOM characteristics

The cDOM absorption spectra between 250 and 700 nm follow different patterns on Herschel Island and Cape Bounty (Fig. 2, Table 2). Absorption is significantly higher ($p < 0.05$) on Herschel Island than on Cape Bounty across the entire spectrum. The absorption at 350 nm wavelength (Fig. 2b) is significantly higher ($p < 0.01$) on Herschel Island (14.5 ± 5.1 m^{-1}) than on Cape Bounty (5.5 ± 4.9 m^{-1}). S275-295 amounts to 16.4 ± 1.5 x 10^{-1} nm^{-1} on Herschel Island and 14.8 ± 3.2 x 10^{-1} nm^{-1} on Cape Bounty.

We found a significant positive relationship ($rho = 0.78$, $p < 0.05$) between the cDOM absorption at 350 nm and DOC concentration for all samples at both sites (Fig. 3a). Average DOC concentrations in surface water samples from Herschel Island amounted to 10.0 ± 1.6 mg l^{-1}, which is significantly higher than on Cape Bounty (2.5 ± 2.0 mg l^{-1}). Comparing the rivers on Herschel Island (Fig. 3b), highest DOC and $a_{cDOM}350$ values were found in the headwaters of Ice Creek West. Ice Creek West had significantly higher ($p < 0.05$) values in DOC (10.4 ± 1.5 mg l^{-1}) and $a_{cDOM}350$ (16.1 ± 5.4 m^{-1}) than Ice Creek East, which were 8.7 ± 1.1 mg l^{-1} and 11.1 ± 1.8 m^{-1}, respectively. No significant difference was found between the SUVA values for the two creeks. The relationship between $a_{cDOM}350$ and DOC at Cape Bounty is broadly separated into two groups, namely flowing and standing water. Both correlations are significant (< 0.05) and show different slopes of the regression (Fig. 3c). DOC and SUVA are significantly different for standing water relative to flowing water. No significant difference between these water types was found for $a_{cDOM}350$. Within the group of standing water, samples from the East River catchment show the highest DOC and $a_{cDOM}350$ values. The highest values of DOC and $a_{cDOM}350$ values of flowing water were recorded in West River after the August 8 rainfall event.

Compared to the SUVA values, we found a moderate negative relationship between SUVA and the mean S275-295 of all water samples from both locations ($rho = -0.64$, $p < 0.05$, Fig. 4a). S275-295 on Herschel Island showed a narrow spread (Fig. 4b) with a clear negative relationship ($rho = -0.72$, $p < 0.05$). The headwaters in both rivers showed slightly smaller slopes than the samples taken downstream. Samples from Cape Bounty (Fig. 4c) showed a negative relationship ($rho = -0.66$, $p < 0.05$) between SUVA and S275-295. Standing water samples showed significantly larger slopes ($p < 0.05$) and significantly smaller SUVA ($p < 0.05$) than flowing water samples.

4.3. Downstream DOM patterns along longitudinal transects

The studied rivers on Herschel Island and Cape Bounty followed different hydrochemical patterns from upstream to downstream (Fig. 5). At Herschel Island, DOC concentration (Fig. 5a) decreased from upstream to downstream for Ice Creek West at all times of sampling, whereas it varies very little from upstream to downstream in Ice Creek East. On 30 July 2016, when both rivers were sampled simultaneously, Ice Creek East showed significantly lower ($p < 0.05$) DOC concentrations than Ice Creek West throughout the entire profile. At ~1300 m from the outflow, Ice Creek West shows a slight increase in DOC

7

concentration. At Cape Bounty, DOC concentrations remain at a similar level (< 2 mg l^{-1}) in all streams, except after the rainfall event in West River. Here, we found higher levels of DOC compared to other Cape Bounty rivers, and also a more pronounced downstream increase of DOC. East River shows a slight downstream decrease of DOC. In Robin Creek, we found an increase in DOC from 1.3 mg l^{-1} to 1.7 mg l^{-1} as the stream gets impacted by a retrogressive thaw slump. DOC drops directly thereafter. Boundary river shows similar concentrations to Robin Creek.

Similar patterns as for DOC were found for a$_{cDOM}$350. This confirms the strong relationship between both parameters (Fig. 3) which is especially high at Herschel Island. At Cape Bounty a$_{cDOM}$350 followed the same pattern as DOC in West River. For the remaining rivers, a$_{cDOM}$350 remained with little variation throughout the profiles.

SUVA values showed different trends in the rivers of Herschel Island and Cape Bounty (Fig. 5c). At Herschel Island, SUVA values remained at the same level along the profiles of both streams and did not show strong differences between rainfall and post rainfall conditions. They follow similar patterns as DOC concentrations and a$_{cDOM}$350. In contrast, at Cape Bounty, West River (sampled after rainfall) showed higher SUVA than the remaining rivers (sampled before the rainfall). Further, an increase in SUVA downstream was visible in Robin Creek and Boundary River, although the number of available data points is limited.

Slope values (S275-295) at Herschel Island were variable in the headwaters and showed an increase downstream (Fig. 5d). They were smallest after the first rainfall event in Ice Creek West and increase progressively over the course of the season. We found lows in the headwaters of Ice Creek West at ~2000 and ~1250m distance from the outflow. Overall, Ice Creek West showed smaller slope values along the stream profile compared to Ice Creek East on 30 July 2016. The rivers on Cape Bounty showed highest slopes for East River ($16.1 \pm 1.6 \times 10^{-3}$ nm^{-1}) and the lowest for West River ($11.9 \pm 0.8 \times 10^{-3}$ nm^{-1}). Robin Creek showed a decrease in slope from 16.8×10^{-3} nm^{-1} at ~2100 m distance to 13.4×10^{-1} nm^{-1} at the outflow. In contrast, a slight downstream increase in slope was recorded in West River.

Electrical conductivity increased from upstream to downstream in Ice Creek West, whereas it remained at a similar level in Ice Creek East (Fig. 5e). It remained below 200 µS cm^{-1} at all times, except for the upstream location in Robin Creek where an active retrogressive thaw slump is hydrologically connected to the stream. It decreased substantially thereafter.

4.4 Temporal trends of DOM with changing meteorological conditions

Changes in discharge, DOM composition and conductivity over the summer season were observed for both rivers at Herschel Island. Rainfall response is direct with steep rising hydrographs and elongated falling limbs (Fig. 6a) in both streams (detailed presentation of rainfall response in Coch et al. 2018). After the peakflow following the 33.9 mm rainfall event (Event-1), both streams showed a decline in DOC accompanied by a decline in a$_{cDOM}$350, SUVA, and an increase in S275-295 (Fig. 6b-e). EC is steadily increasing after peakflow in both streams (Fig. 6f).

The subsequent rainfall event (Event-2, 9.3 mm) led to an increase of DOC, a$_{cDOM}$350 and S275-295, and a decrease in SUVA (Fig. 6b-e) in Ice Creek West. This dynamic was not captured in Ice Creek East, which was sampled at a longer time interval. Baseflow had increased after this rainfall event (Fig. 6a).

The hydrochemical response to rainfall Event-3 (12.7 mm) was different than the response to Event-2. An initial decrease in DOC, $a_{cDOM}350$ and S275-295 is followed by a sharp increase of these parameters in Ice Creek West. SUVA increases with two spikes in the data. Ice Creek East had a different response showing an increase in DOC and $a_{cDOM}350$ and a drop in SUVA. The scale depicts only S275-295 values below 18×10^{-3} nm^{-1} to capture the variability, hence the two gaps in the Ice Creek East data.

5 Discussion

5.1 Limitations of cDOM measurements from terrestrial sources

There are a few constraints to optical DOM measurements and the samples themselves that we encountered in this study. As described in the methods section, some samples formed precipitates inside the bottles in the form of small thin flakes, which partly remained in suspension or accumulated at the bottom. All samples were filtered in the field through 0.7 µm glass fiber filters, and the precipitation occurred after filtration during storage. At Cape Bounty, these problematic samples had very high a_{cDOM} values of 13.9 ± 13.8 m^{-1} with a maximum of 75.8 m^{-1}, and SUVA values of 10.1 ± 11.5 L mg^{-1} m^{-1} with a maximum of 59.5 L mg^{-1} m^{-1}. Those values are significantly higher (p <0.05) than the mean values reported in Table 2 and are not realistic for natural surface waters. At Herschel Island, a_{cDOM} and SUVA did not differ significantly from the mean (11.8 ± 0.8 m^{-1} and 3.5 ± 0.4 L mg^{-1} m^{-1} respectively). As described in the methods section (3.1), samples showing precipitates in the laboratory were excluded from the study, even if the absorption values were plausible when compared to the corresponding DOC concentration (Fig 7). At Cape Bounty, this was the case for 25 out of 55 samples. We assume that absorbance measurements are high as a result of scattering by newly formed colloid complexes and precipitates. Also, Hansen et al. (2016) and Weishaar et al. (2003) report that SUVA values above 6.0 L mg^{-1} m^{-1} are indicative for absorption from other constituents in the sample (Hansen et al., 2016; Weishaar et al., 2003).

We assume that the absorption interference could be due to polymeric iron (hydr)oxides or high concentrations of dissolved iron. Dissolved iron in terrestrially dominated waters is dominantly complexed with humic and fulvic acids. Therefore, with changing temperature and changing pH of the sample filtrates, redox reaction can result in colloid formation and phase changes, which then strongly affect the optical properties of the sample filtrate by scattering. Poulin et al (2014) describe how iron (Fe(II,III)) is known to interfere with the absorption of cDOM with a linear dependency of increasing a_{cDOM} with increasing Fe(III) concentration in the water. Poulin et al. (2014) suggest to correct cDOM absorption coefficients according to the iron concentrations using correction coefficients. Coch et al. (2018) report total aqueous dissolved iron concentrations from Herschel Island. High total iron concentration is found to occur in high $a_{cDOM}350$ (Fig. S2), which indicates a potential influence of iron concentration on the absorption. Fraction of Fe(II) and Fe(III) on the total iron concentration was not measured as a standard hydrochemistry measurement, thus the correction could not be performed. However, Figure 7 clearly shows that the samples that were removed fell into the problematic group (circled), where cDOM was overestimated compared to DOC concentration. This conservative approach removed also other samples with reasonable cDOM to DOC ratios.

5.2 Nature of the cDOM to DOC relationship across the terrestrial Arctic

Strong positive correlations between DOC and $a_{cDOM}350$ as found in this study (Fig. 3a) were previously reported in the large Arctic rivers (Walker et al., 2013) and globally (Massicotte et al., 2017). DOC and cDOM values are available from surface waters in northeastern Canada (Breton et al., 2009), Scandinavia (Forsström et al., 2015; Kellerman et al., 2015) and the Alaskan Arctic (Cory et al., 2015; Larouche et al., 2015). Comparing our sites to those found in the literature confirms the strong positive relationship (rho = 0.85, p < 0.05) between DOC and $a_{cDOM}350$ (Fig. S3), indicating the robustness for using the optical parameter a_{cDOM} as a proxy for DOC concentration in terrestrial freshwater systems. However, this relationship holds not true for sites where dissolved organic matter is strongly altered, for example through photodegradation (Osburn et al., 2017).

We linked cDOM and $a_{cDOM}350$ from this study and the literature (Table 3; Supplementary Table S1, S2) to latitude and the soil organic carbon content (SOCC) in 0-30 cm and 0-100 cm depth as retrieved from Hugelius et al. (2013). We found a positive correlation (rho = 0.53/0.51, p < 0.05) between SOCC and DOC concentration. The relationship between $a_{cDOM}350$ and SOCC is also significant, although weaker (rho = 0.26 / 0.34, p < 0.05). It is important to bear in mind that the northern circumpolar soil carbon database is a product of upscaling and will most likely not cover the spatial variability reported in the studies. Nevertheless, the data shows a decrease of SOCC at higher latitudes, influenced by climate to a certain degree. DOM and SOCC are further linked to watershed slope: Longer residence times in low relief terrain and high hydrologic connectivity facilitate leaching and export of DOM from soil organic matter (Connolly et al., 2018; Harms et al., 2016). Also, several of the studies contain data on lakes in large river floodplains with very large catchment sizes. For example, Skorospekhova et al. (2016) report high cDOM and DOC concentrations for tundra lakes in the Lena Delta, which are influenced by the spring flood delivering organic material into the lakes.

Walker et al. (2013) report SUVA for three different flow regimes of the large Arctic rivers: peakflow (spring freshet), midflow (summer) and baseflow (winter). The SUVA values reported in this study (2.9 ± 0.4 L mg^{-1} m^{-1} for Herschel Island and 2.8 ± 1.1 L mg^{-1} m^{-1} for Cape Bounty) are higher than the mean mid-flow SUVA for the five Arctic rivers (2.4 L mg^{-1} m^{-1}), which ranges between 2.0 L mg^{-1} m^{-1} in the Mackenzie River and 2.7 L mg^{-1} m^{-1} in the Ob'. This confirms the hypothesis proposed by Vonk et al. (2015b), that DOM exported from smaller rivers has a higher aromaticity, which suggests that the material is fresh (less altered) and prone to degradation. The large Arctic rivers cover approximately half of the Arctic drainage basin, whereas the other half is covered by smaller catchments. Although the exact size distribution remains unknown, our results suggest that these smaller rivers could potentially deliver material that is "fresher" and more prone to degradation, compared to the large Arctic rivers.

5.3 Catchment processes and biogeochemical cycling

5.3.1 Regional catchment properties

Our study sites show strong differences in DOM quantity and quality possibly related to their geographic location and environmental setting. Herschel Island (Low Arctic) shows on average significantly higher values in DOC, $a_{cDOM}350$, and SUVA than Cape Bounty (High Arctic). Although catchment slope is an important driver of DOC concentrations (Connolly et al., 2018), also vegetation type and soil characteristics play an important role (Harms et al., 2016). Greater abundance of plant material in the Low Arctic (Fig. 1) results in high lignin concentration that can be introduced into the aquatic system (Sulzberger and Durisch-Kaiser, 2009), resulting in high DOC and $a_{cDOM}350$ values.

The variability and range of SUVA and S275-295, indicating the molecular weight and aromaticity, is greater on Cape Bounty than it is on Herschel Island. The greater ranges of SUVA and S275-295 at Cape Bounty indicates a greater variability of DOM quality there. High SUVA in combination with low S275-295 indicate "fresh" DOM, or systems of shorter residence time receiving a greater input of fresh DOM from the catchment area. In contrast, low SUVA and high S275-195 might be an indicator of limited fresh DOM inputs, a higher relative contribution of autochthonous DOM, greater exposure to photobleaching and longer residence time (Anderson and Stedmon, 2007; Fichot and Benner, 2012; Fichot et al., 2013; Helms et al., 2008; Whitehead et al., 2000).

At Cape Bounty, two different water types were identified based on the cDOM to DOC ratios (Fig. 3c). Group 1, dominated by standing water bodies, showed lower cDOM to DOC ratios compared to group 2. We explain this difference in ratios by different turbidity and residence times. In surface waters photodegradation of DOM is a dominant process (Vonk et al., 2015b). Short residence times, but specifically turbidity through sediment inputs or resuspension might limit photodegradation processes (Cory et al., 2015; Cory et al., 2014).

5.3.2 Rainfall events

Rain magnitude, intensity and antecedent conditions play an important role for mobilizing DOM from permafrost catchments. At Herschel Island, we captured the response to three different rainfall events through continuous sampling at the outflow and repeated sampling along the longitudinal stream profile in Ice Creek West. Rainfall Event-1 (33.9 mm) was captured only at the receding hydrograph at the outflow (Fig. 6), but along the stream profile in Ice Creek West (Fig. 5). This event of high magnitude and intensity led to high SUVA and low S275-295 values indicating "fresh" plant derived DOM that is prone to degradation. After this event, the hydrograph recedes, and the DOM signature during the "post rain" conditions suggests a sourcing from deeper in the active layer (decreasing SUVA and increasing S275-295 at the outflow and throughout the profile). The contrasting response of Ice Creek West to rainfall events 2 and 3, suggests different sourcing of DOM and controlling factors. During the second rainfall event (9.3 mm), as DOC increased, we found a decrease in SUVA accompanied by an increase in S275-295. This indicates a decrease in aromaticity and a lower molecular weight, indicative of more decomposed material. The following event of 12.7 mm led to a decrease in DOC and S275-295 and an increase in SUVA indicating an

increase in aromaticity and a higher molecular weight – suggesting more lignin rich plant derived DOM. A change in water sources for these two rainfall events was examined by Coch et al. (in review). Whereas runoff during the 9.3 mm rainfall event showed the signature of supra-permafrost water, which was forced out during that rainfall event, runoff during the subsequent 12.7 mm rainfall event reflected the isotopic signature of rain. Thus, the DOM was first sourced from the surface and through

5   the entire active layer and had a longer residence time than the rain event after. This indicates that antecedent (pre-rainfall) conditions play a crucial role for the sourcing of DOM. The second rainfall event (9.3 mm) occurred about 10 days after the first one (33.9 mm), whereas the time difference between the second and the third one was less than 4 days. In addition to the antecedent conditions, the magnitude and intensity of the rainfall event might also play an important role here. The 9.3 mm rainfall event occurred over a period of 3 days. Thus, the flow pathways during this event might be deeper in the active layer

10   mobilizing more decomposed OM (Marín-Spiotta et al., 2014). In contrast, the subsequent 12.7 mm event occurred within 1 day, which presumably led to increased overland flow and the mobilization of surface OM. Baseflow in this catchment is increasing with summer rainfall and as the summer season progresses (Coch et al., 2018). The authors also reported a linear increase of DOC export with increasing runoff. Our dataset shows that the quality of exported DOC depends on the intensity of rainfall and the antecedent conditions, which in turn determine hydrological flow pathways and sourcing of DOM.

15   Although only one river was sampled before and after rainfall on Cape Bounty (West River), we found a substantial increase in DOC there compared to the pre-rainfall concentrations. Fouché et al. (2017) conducted an extensive study of DOM quality in four headwater streams of West River (Cape Bounty) and also reported an increase in DOC concentrations and fluxes during stormflow. They observed a change in DOM quality: enrichment in fresh low molecular weight (LMW), microbially-derived, components as indicated by an increase in S275-295 and a decrease in SUVA during rainfall. Although we do not have data

20   on the optical properties for West River before the rainfall event, similar concentrations of DOC in West River and East River point towards similar optical characteristics at that time. Baseflow in undisturbed High Arctic headwater streams seems therefore characterized by more high molecular weight (HMW) humic-like components with high aromaticity (low slope and increase in SUVA) relative to stormflow DOM. In turn, stormflow leads to an export of DOM characterized by lower molecular weight and decreased aromaticity (high slope, decreased SUVA). Fouché et al. (2017) explain this pattern by a change in flow

25   pathways from shallow active layer soils (baseflow) to subsurface runoff (rainfall), where soluble components from mineral soils deeper in the active layer are mobilized. Associated with the change in DOM quality, they also found an increase in total dissolved solids (TDS) supporting this hypothesis. Impacts of changing flow pathways on DOM quality are also reported from a Subarctic setting by Balcarczyk et al. (2009). The increased residence time of percolating water through the active layer leads to a selective sorption of compounds to mineral soil particles. The authors describe that hydrophobic compounds are absorbed,

30   while hydrophilic compounds remain in the solution, and are therefore exported from the catchment (Balcarczyk et al., 2009). Further, an increased residence time and subsurface flow mobilizes DOC that is more microbially degraded (Striegl et al., 2005; Ward and Cory, 2015).

Different studies anticipate a shift towards deeper flow pathways as active layer depths increase with climate change (Drake et al., 2018; Mann et al., 2015; O'Donnell et al., 2014; Ward and Cory, 2015). These studies found that permafrost-derived

DOM is more labile compared to surface (organic mat) DOM. As described above, we show that stormflow at the Low and High Arctic locations alter flow pathways and therefore the quality of DOM exported. At the Low Arctic setting our data suggests that more permafrost-derived DOM is exported with increasing baseflow during the season and during a rainfall event of smaller magnitude and lower intensity. Based on the optical properties, this material shows low molecular weight and aromaticity, i.e. it is already altered and not prone to degradation. In contrast, rainfall events of high magnitude and intensity that act on saturated soil lead to shorter residence time in the flow path and thus export more fresh (less altered) near-surface-derived DOM (higher SUVA and lower S275-295). As summer rainfall is projected to increase across the Arctic (Bintanja, 2018; Bintanja and Andry, 2017), we are expecting an increase in DOC export (Coch et al. 2018). Small catchments in the subarctic Canadian Shield already shift towards a nival-pluvial flow regime leading to substantial increases in organic matter fluxes during fall and winter (Spence et al., 2011; Spence et al., 2015). The DOM quality will depend on the residence time and thus, flow pathways within the catchment, which in turn is controlled by the frequency and magnitude of the rainfall events and the thaw depth of the active layer.

5.3.3 Downstream patterns and impact of permafrost disturbance

Transport and degradation of DOC is a dynamic process. Vonk et al. (2015b) showed that the degradability decreased from small streams towards larger rivers within the continuous permafrost zone. The fate of DOC along lateral flow pathways from headwater streams through lakes and large rivers to the ocean is connected to photochemical and biological oxidation (Cory et al., 2015; Cory et al., 2014). Studies show the importance of headwater systems where photodegradation (Cory et al., 2014) and bacterial respiration of ancient permafrost-derived DOC are prevalent (Mann et al., 2015). Our objective was therefore to investigate the upstream to downstream patterns in small coastal catchments in the Low and High Arctic.

At Herschel Island, we found a high variability of DOC, SUVA and S275-295 in the headwaters of Ice Creek West. The locations at 2000 m and 1300 m distance from the outflow show high DOC, S275-295 and low SUVA compared to the other locations. This is due to degrading ice-wedge polygons, which heavily influence DOM in the headwaters of the stream (Coch et al. in review). The location at 1300 m marks the inflow of another headwater tributary impacted by degrading ice-wedge polygons. Thus, main expected sources for fresh mobilized DOM are headwaters and water from the tributary. DOC and $a_{cDOM}350$ show highest values in the headwaters decreasing towards the outflow. Increasing S275-295 along both streams stream is indicative of a gradual photochemical degradation of DOM with distance. S275-295 has been found a good indicator for photodegradation of DOM (Fichot and Benner, 2012; Fichot et al., 2013; Helms et al., 2008), and also been observed along a flow-path continuum of the Kolyma river basin (Frey et al., 2016). Here, they found a relative constant proportion of bioavailable DOM along the entire flow path, indicating an acclimatization of aquatic microorganisms to downstream DOM changes and/or the generation of labile DOM for microbial processing through photodegradation. SUVA values show a similar pattern to DOC and $a_{cDOM}350$ including the distinct increase at 1300 m. Cory et al. (2014, 2015) show at a Subarctic site that DOC in headwater streams, which are directly sourced by soil water, have low prior exposure to light and is therefore prone to photodegradation to CO_2. The temporal variation of the DOM parameters across the stream profile is in line the onset

At Cape Bounty, optical data of upstream to downstream patterns is more limited (see section 5.3). West River shows an increase in DOC downstream (3 August 2017), which is also reflected in an increase of $a_{cDOM}350$. As discussed by Fouché et al. (2017) and Wang et al. (2018), West River is characterized by a downstream increase in autochthonous DOM. SUVA and S275-295 do not show strong differences downstream in the West River suggesting little modification of DOM through microbial and/or photodegradation processes. A retrogressive thaw slump at Robin Creek heavily impacts DOM quality. At ~2100 m distance from the outflow, closest to the slump, we see the highest DOC, S275-295 and EC values and lowest SUVA. This is indicative of low aromaticity and lower molecular weight. Abbott et al. (2014) found that DOM is most biodegradable during active disturbance at sites in the Subarctic. SUVA values at thermokarst outflows in that study are half as high as in undisturbed reference waters indicating less aromatic DOC. High S275-295 and SR were observed in conjunction with geomorphic disturbance in headwater streams of West River by Fouché et al. (2017). Impact of retrogressive thaw slumps on DOM quality was also studied in the Subarctic Peel Plateau by Littlefair et al. (2017). They reported similar dynamics at modestly sized slumps as we observed at Robin Creek: DOC concentration is highest directly at the slump outflow and is lower downstream compared to the undisturbed site before the slump impacted the stream. The authors attribute low SUVA and high S275-295 within the disturbed site to deep permafrost flow pathways. Our SUVA values within the slump and downstream are very similar to the ones reported by Littlefair et al. (2017), despite the great geographical difference.

6 Conclusion

This study investigates DOM optical properties in Low and High Arctic surface water environments and downstream patterns with regard to permafrost disturbance and rainfall events. We find that both Arctic locations exhibit a distinct signature of DOC concentration and $a_{cDOM}350$ linked to the differences in vegetation cover and SOCC content. Compared to the High Arctic, $a_{cDOM}350$ in the Low Arctic is higher due to the greater abundance of plant material and higher lignin concentrations introduced into the aquatic system. SOCC is higher in the Low Arctic than in the High Arctic. This results in higher DOC and $a_{cDOM}350$ values in the Low Arctic (Herschel Island) than in the High Arctic (Cape Bounty).

In both regions, the strong terrestrial signature of DOM is apparent in the optical properties, which is typical for small headwater catchments. The relationship between $a_{cDOM}350$ and DOC is very strong across both regions and including data from the literature, proving the applicability of cDOM as a tracer for DOC throughout different aquatic Arctic environments (rivers, streams and lakes). However, examining DOM optical characteristics (SUVA, S275-295 and SR) for those large rivers and our sites, we find that smaller catchments in our study deliver fresh, less altered DOM prone to degradation.

The optical characteristics of DOM prove also a useful tool for assessing downstream patterns in the streams studied. The downstream increase of S275-295 is indicative for photodegradation processes, which is apparent in most of the streams. Although the temporal resolution of data at Cape Bounty is limited, we found a similar response to rainfall events. Rainfall leading to runoff with a short residence time (rainfall of high magnitude and intensity, dry antecedent conditions in the catchment) leads to the export of fresh near-surface-derived DOM (higher SUVA, lower S275-295). In contrast, baseflow

conditions and long residence times (including low magnitude rainfall events and a saturated catchment) favors the export of permafrost-derived DOM that has undergone microbial processing in the soil. Examining flow pathways and residence time will be crucial to assess the impacts of projected increasing summer rainfall across the Arctic. Optical properties of DOM will be a useful tool for assessing DOM quality changes at a pan-Arctic scale.

5

Competing interests

The authors declare that they have no conflict of interest.

References

Abbott, B. W., Larouche, J. R., Jones, J. B., Bowden, W. B., and Balser, A. W.: Elevated dissolved organic carbon biodegradability from thawing and collapsing permafrost, J Geophys Res Biogeosci, 119, 2049-2063, 10.1002/2014jg002678, 2014.

ADAPT: Carbon, nitrogen and water content of the active layer from sites across the Canadian Arctic Nordicana D21, 10.5885/45327AD-5245D08606AB4F52, 2014.

Aiken, G. R.: Fluorescence and dissolved organic matter: A chemist's perspective: Chapter 2, 35-74, 10.1017/CBO9781139045452.005, 2014.

Anderson, N. J., and Stedmon, C. A.: The effect of evapoconcentration on dissolved organic carbon concentration and quality in lakes of SW Greenland, Freshw. Biol., 52, 280-289, 10.1111/j.1365-2427.2006.01688.x, 2007.

Balcarczyk, K. L., Jones, J. B., Jaffé, R., and Maie, N.: Stream dissolved organic matter bioavailability and composition in watersheds underlain with discontinuous permafrost, Biogeochemistry, 94, 255-270, 10.1007/s10533-009-9324-x, 2009.

Bintanja, R., and Andry, O.: Towards a rain-dominated Arctic, Nat Clim Chang, 7, 263-267, 10.1038/nclimate3240, 2017.

Bintanja, R.: The impact of Arctic warming on increased rainfall, Sci. Rep., 8, 16001, 10.1038/s41598-018-34450-3, 2018.

Breton, J., Prairie, Y., Vallières, C., and Laurion, I.: Limnological properties of permafrost thaw ponds in northeastern Canada, Can. J. Fish. Aquat. Sci., 66, 1635-1648, 10.1139/f09-108, 2009.

Burn, C. R.: Herschel Island Qikiqtaryuk: A Natural and Cultural History of Yukon's Arctic Island, edited by: Burn, C. R., University of Calgary Press, 242 pp., 2012.

CAVM: Circumpolar Arctic Vegetation Map, Conservation of Arctic Flora and Fauna (CAFF) Map, 2003.

Coch, C., Lamoureux, S. F., Knoblauch, C., Eischeid, I., Fritz, M., Obu, J., and Lantuit, H.: Summer rainfall DOC, solute and sediment fluxes in a small Arctic coastal catchment on Herschel Island (Yukon Territory, Canada), Arctic Science, 10.1139/as-2018-0010, 2018.

Coch, C., Ramage, J. L., Lamoureux, S., Knoblauch, C., Meyer, H., and Lantuit, H.: Spatial variability of dissolved organic carbon (DOC), solutes and suspended sediment in disturbed Low Arctic coastal watersheds. , Journal of Geophysical Research: Biogeosciences (in review), in review.

Connolly, C. T., Khosh, M. S., Burkart, G. A., Douglas, T. A., Holmes, R. M., Jacobson, A. D., Tank, S. E., and McClelland, J. W.: Watershed slope as a predictor of fluvial dissolved organic matter and nitrate concentrations across geographical space and catchment size in the Arctic, Environ Res Lett, 13, 10.1088/1748-9326/aae35d, 2018.

Cory, R. M., Ward, C. P., Crump, B. C., and Kling, G. W.: Carbon cycle. Sunlight controls water column processing of carbon in arctic fresh waters, Science, 345, 925-928, 10.1126/science.1253119, 2014.

Cory, R. M., Harrold, K. H., Neilson, B. T., and Kling, G. W.: Controls on dissolved organic matter (DOM) degradation in a headwater stream: the influence of photochemical and hydrological conditions in determining light-limitation or substrate-limitation of photo-degradation, Biogeosciences, 12, 6669-6685, 10.5194/bg-12-6669-2015, 2015.

Drake, T. W., Tank, S. E., Zhulidov, A. V., Holmes, R. M., Gurtovaya, T., and Spencer, R. G. M.: Increasing Alkalinity Export from Large Russian Arctic Rivers, Environ. Sci. Technol., 52, 8302-8308, 10.1021/acs.est.8b01051, 2018.

Dvornikov, Y., Leibman, M., Heim, B., Bartsch, A., Herzschuh, U., Skorospekhova, T., Fedorova, I., Khomutov, A., Widhalm, B., Gubarkov, A., and Rößler, S.: Terrestrial CDOM in Lakes of Yamal Peninsula: Connection to Lake and Lake Catchment Properties, Remote Sensing, 10, 10.3390/rs10020167, 2018.

Edwards, R., and Treitz, P.: Vegetation Greening Trends at Two Sites in the Canadian Arctic: 1984–2015, Arct. Antarct. Alp. Res., 49, 601-619, 10.1657/aaar0016-075, 2018.

Environment and Climate Change Canada, Historical Data: http://climate.weather.gc.ca/historical_data/search_historic_data_e.html, access: 12 December 2018, 2018.

Fichot, C. G., and Benner, R.: The spectral slope coefficient of chromophoric dissolved organic matter (S 275-295) as a tracer of terrigenous dissolved organic carbon in river-influenced ocean margins, Limnol. Oceanogr., 57, 1453-1466, 10.4319/lo.2012.57.5.1453, 2012.

Fichot, C. G., Kaiser, K., Hooker, S. B., Amon, R. M., Babin, M., Belanger, S., Walker, S. A., and Benner, R.: Pan-Arctic distributions of continental runoff in the Arctic Ocean, Sci. Rep., 3, 1053, 10.1038/srep01053, 2013.

Forsström, L., Rautio, M., Cusson, M., Sorvari, S., Albert, R.-L., Kumagai, M., and Korhola, A.: Dissolved organic matter concentration, optical parameters and attenuation of solar radiation in high-latitude lakes across three vegetation zones, Ecoscience, 22, 17-31, 10.1080/11956860.2015.1047137, 2015.

Fouché, J., Lafrenière, M. J., Rutherford, K., and Lamoureux, S.: Seasonal hydrology and permafrost disturbance impacts on dissolved organic matter composition in High Arctic headwater catchments, Arctic Science, 3, 378-405, 10.1139/as-2016-0031, 2017.

Frey, K. E., and Smith, L. C.: Amplified carbon release from vast West Siberian peatlands by 2100, Geophys. Res. Lett., 32, 10.1029/2004gl022025, 2005.

Frey, K. E., Sobczak, W. V., Mann, P. J., and Holmes, R. M.: Optical properties and bioavailability of dissolved organic matter along a flow-path continuum from soil pore waters to the Kolyma River mainstem, East Siberia, Biogeosciences, 13, 2279-2290, 10.5194/bg-13-2279-2016, 2016.

Green, S. A., and Blough, N. V.: Optical absorption and fluorescence properties of chromophoric dissolved organic matter in natural waters, Limnol. Oceanogr., 39, 1903-1916, 10.4319/lo.1994.39.8.1903, 1994.

Hansen, A. M., Kraus, T. E. C., Pellerin, B. A., Fleck, J. A., Downing, B. D., and Bergamaschi, B. A.: Optical properties of dissolved organic matter (DOM): Effects of biological and photolytic degradation, Limnol. Oceanogr., 61, 1015-1032, 10.1002/lno.10270, 2016.

Harms, T. K., Edmonds, J. W., Genet, H., Creed, I. F., Aldred, D., Balser, A., and Jones, J. B.: Catchment influence on nitrate and dissolved organic matter in Alaskan streams across a latitudinal gradient, J Geophys Res Biogeosci, 121, 350-369, 10.1002/2015jg003201, 2016.

Helms, J. R., Stubbins, A., Ritchie, J. D., Minor, E. C., Kieber, D. J., and Mopper, K.: Absorption spectral slopes and slope ratios as indicators of molecular weight, source, and photobleaching of chromophoric dissolved organic matter, 2008.

Hodgson, D. A., Vincent, J. S., and Fyles, J. G.: Quaternary geology of central Melville Island, Northwest Territories. Geological Survey of Canada, 10.4095/119784, 1984.

Holmes, R. M., McClelland, J. W., Peterson, B. J., Tank, S. E., Bulygina, E., Eglinton, T. I., Gordeev, V. V., Gurtovaya, T. Y., Raymond, P. A., Repeta, D. J., Staples, R., Striegl, R. G., Zhulidov, A. V., and Zimov, S. A.: Seasonal and Annual Fluxes of Nutrients and Organic Matter from Large Rivers to the Arctic Ocean and Surrounding Seas, Estuar. Coasts, 35, 369-382, 10.1007/s12237-011-9386-6, 2012.

Hugelius, G., Tarnocai, C., Broll, G., Canadell, J. G., Kuhry, P., and Swanson, D. K.: The Northern Circumpolar Soil Carbon Database: spatially distributed datasets of soil coverage and soil carbon storage in the northern permafrost regions, Earth System Science Data, 5, 3-13, 10.5194/essd-5-3-2013, 2013.

Hugelius, G., Strauss, J., Zubrzycki, S., Harden, J. W., Schuur, E. A. G., Ping, C. L., Schirrmeister, L., Grosse, G., Michaelson, G. J., Koven, C. D., amp, apos, Donnell, J. A., Elberling, B., Mishra, U., Camill, P., Yu, Z., Palmtag, J., and Kuhry, P.: Estimated stocks of circumpolar permafrost carbon with quantified uncertainty ranges and identified data gaps, Biogeosciences, 11, 6573-6593, 10.5194/bg-11-6573-2014, 2014.

Kellerman, A. M., Kothawala, D. N., Dittmar, T., and Tranvik, L. J.: Persistence of dissolved organic matter in lakes related to its molecular characteristics, Nat. Geosci., 8, 454-457, 10.1038/ngeo2440, 2015.

Lacelle, D., Bjornson, J., and Lauriol, B.: Climatic and geomorphic factors affecting contemporary (1950-2004) activity of retrogressive thaw slumps on the Aklavik Plateau, Richardson Mountains, NWT, Canada, Permafr. Periglac. Proc., 21, 1-15, 10.1002/ppp.666, 2010.

Lafrenière, M. J., and Lamoureux, S. F.: Thermal Perturbation and Rainfall Runoff have Greater Impact on Seasonal Solute Loads than Physical Disturbance of the Active Layer, Permafr. Periglac. Proc., 24, 241-251, 10.1002/ppp.1784, 2013.

Lafrenière, M. J., Laurin, E., and Lamoureux, S. F.: The Impact of Snow Accumulation on the Active Layer Thermal Regime in High Arctic Soils, Vadose Zone J., 12, 10.2136/vzj2012.0058, 2013.

Lamoureux, S. F., and Lafrenière, M. J.: Fluvial Impact of Extensive Active Layer Detachments, Cape Bounty, Melville Island, Canada, Arct. Antarct. Alp. Res., 41, 59-68, 10.1657/1938-4246(08-030)[lamoureux]2.0.co;2, 2009.

Lamoureux, S. F., and Lafrenière, M. J.: More than just snowmelt: integrated watershed science for changing climate and permafrost at the Cape Bounty Arctic Watershed Observatory, WIREs Water, 5, e1255, 10.1002/wat2.1255, 2017.

Lantuit, H., and Pollard, W. H.: Fifty years of coastal erosion and retrogressive thaw slump activity on Herschel Island, southern Beaufort Sea, Yukon Territory, Canada, Geomorphology, 95, 84-102, 10.1016/j.geomorph.2006.07.040, 2008.

Larouche, J. R., Abbott, B. W., Bowden, W. B., and Jones, J. B.: The role of watershed characteristics, permafrost thaw, and wildfire on dissolved organic carbon biodegradability and water chemistry in Arctic headwater streams, Biogeosciences, 12, 4221-4233, 10.5194/bg-12-4221-2015, 2015.

Le Fouest, V., Matsuoka, A., Manizza, M., Shernetsky, M., Tremblay, B., and Babin, M.: Towards an assessment of riverine dissolved organic carbon in surface waters of the western Arctic Ocean based on remote sensing and biogeochemical modeling, Biogeosciences, 15, 1335-1346, 10.5194/bg-15-1335-2018, 2018.

Lewis, T., Lafrenière, M. J., and Lamoureux, S. F.: Hydrochemical and sedimentary responses of paired High Arctic watersheds to unusual climate and permafrost disturbance, Cape Bounty, Melville Island, Canada, Hydrol. Processes, 26, 2003-2018, 10.1002/hyp.8335, 2012.

Lewkowicz, A. G.: Dynamics of active-layer detachment failures, Fosheim Peninsula, Ellesmere Island, Nunavut, Canada, Permafr. Periglac. Proc., 18, 89-103, 10.1002/ppp.578, 2007.

Littlefair, C. A., Tank, S. E., and Kokelj, S. V.: Retrogressive thaw slumps temper dissolved organic carbon delivery to streams of the Peel Plateau, NWT, Canada, Biogeosciences, 14, 5487-5505, 10.5194/bg-14-5487-2017, 2017.

Mackay, J. R.: Glacier ice-thrust features of the Yukon coast, Geographical Bulletin, 13, 5-21, 1959.

Mann, P. J., Davydova, A., Zimov, N., Spencer, R. G. M., Davydov, S., Bulygina, E., Zimov, S., and Holmes, R. M.: Controls on the composition and lability of dissolved organic matter in Siberia's Kolyma River basin, J Geophys Res Biogeosci, 117, 10.1029/2011jg001798, 2012.

5 Mann, P. J., Eglinton, T. I., McIntyre, C. P., Zimov, N., Davydova, A., Vonk, J. E., Holmes, R. M., and Spencer, R. G.: Utilization of ancient permafrost carbon in headwaters of Arctic fluvial networks, Nat Commun, 6, 7856, 10.1038/ncomms8856, 2015.

Marín-Spiotta, E., Gruley, K. E., Crawford, J., Atkinson, E. E., Miesel, J. R., Greene, S., Cardona-Correa, C., and Spencer, R. G. M.: Paradigm shifts in soil organic matter research affect interpretations of aquatic carbon cycling: transcending disciplinary and ecosystem boundaries, Biogeochemistry, 117, 279-297, 10.1007/s10533-013-9949-7, 2014.

10 Massicotte, P., Asmala, E., Stedmon, C., and Markager, S.: Global distribution of dissolved organic matter along the aquatic continuum: Across rivers, lakes and oceans, Sci. Total Environ., 609, 180-191, 10.1016/j.scitotenv.2017.07.076, 2017.

Myers-Smith, I. H., Hik, D. S., Kennedy, C., Cooley, D., Johnstone, J. F., Kenney, A. J., and Krebs, C. J.: Expansion of Canopy-Forming Willows Over the Twentieth Century on Herschel Island, Yukon Territory, Canada, Ambio, 40, 610-623, 10.1007/s13280-011-0168-y, 2011.

Neff, J. C., Finlay, J. C., Zimov, S. A., Davydov, S. P., Carrasco, J. J., Schuur, E. A. G., and Davydova, A. I.: Seasonal changes in the age

15 and structure of dissolved organic carbon in Siberian rivers and streams, Geophys. Res. Lett., 33, 10.1029/2006gl028222, 2006.

O'Donnell, J. A., Aiken, G. R., Walvoord, M. A., Raymond, P. A., Butler, K. D., Dornblaser, M. M., and Heckman, K.: Using dissolved organic matter age and composition to detect permafrost thaw in boreal watersheds of interior Alaska, J Geophys Res Biogeosci, 119, 2155-2170, 10.1002/2014jg002695, 2014.

Osburn, C. L., Anderson, N. J., Stedmon, C. A., Giles, M. E., Whiteford, E. J., McGenity, T. J., Dumbrell, A. J., and Underwood, G. J. C.:

20 Shifts in the Source and Composition of Dissolved Organic Matter in Southwest Greenland Lakes Along a Regional Hydro-climatic Gradient, J Geophys Res Biogeosci, 122, 3431-3445, 10.1002/2017jg003999, 2017.

Osterkamp, T. E.: Characteristics of the recent warming of permafrost in Alaska, J. Geophys. Res., 112, 10.1029/2006jf000578, 2007.

Pollard, W. H.: The nature and origin of ground ice in the Herschel Island area, Yukon Territory, Proceedings, Fifth Canadian Permafrost Conference, Québec, 23-30, 1990.

25 Ramage, J. L., Irrgang, A. M., Morgenstern, A., and Lantuit, H.: Increasing coastal slump activity impacts the release of sediment and organic carbon into the Arctic Ocean, Biogeosciences, 15, 1483-1495, 10.5194/bg-15-1483-2018, 2018.

Ramage, J. L., Fortier, D., Hugelius, G., Lantuit, H., and Morgenstern, A.: Distribution of carbon and nitrogen along hillslopes in three valleys on Herschel Island, Yukon Territory, Canada, Catena, 178, 132-140, 10.1016/j.catena.2019.02.029, 2019.

Schaefer, K., Lantuit, H., Romanovsky, V. E., Schuur, E. A. G., and Witt, R.: The impact of the permafrost carbon feedback on global

30 climate, Environ Res Lett, 9, 085003, 10.1088/1748-9326/9/8/085003, 2014.

Smith, C. A. S., Kennedy, C. E., Hargrave, A. E., and McKenna, K. M.: Soil and vegetation of Herschel Island, Yukon Territory, Ottawa, ON, 101, 1989.

Spence, C., Kokelj, S., and Ehsanzadeh, E.: Precipitation trends contribute to streamflow regime shifts in northern Canada, 3-8 pp., 2011.

Spence, C., Kokelj, S. V., Kokelj, S. A., McCluskie, M., and Hedstrom, N.: Evidence of a change in water chemistry in Canada's subarctic

35 associated with enhanced winter streamflow, J Geophys Res Biogeosci, 120, 113-127, 10.1002/2014jg002809, 2015.

Spencer, R. G. M., Aiken, G. R., Wickland, K. P., Striegl, R. G., and Hernes, P. J.: Seasonal and spatial variability in dissolved organic matter quantity and composition from the Yukon River basin, Alaska, Global Biogeochem. Cycles, 22, n/a-n/a, 10.1029/2008gb003231, 2008.

Spencer, R. G. M., Aiken, G. R., Butler, K. D., Dornblaser, M. M., Striegl, R. G., and Hernes, P. J.: Utilizing chromophoric dissolved organic

40 matter measurements to derive export and reactivity of dissolved organic carbon exported to the Arctic Ocean: A case study of the Yukon River, Alaska, Geophys. Res. Lett., 36, 10.1029/2008gl036831, 2009.

Stedmon, C. A., Amon, R. M. W., Rinehart, A. J., and Walker, S. A.: The supply and characteristics of colored dissolved organic matter (CDOM) in the Arctic Ocean: Pan Arctic trends and differences, Mar. Chem., 124, 108-118, 10.1016/j.marchem.2010.12.007, 2011.

Striegl, R. G., Aiken, G. R., Dornblaser, M. M., Raymond, P. A., and Wickland, K. P.: A decrease in discharge-normalized DOC export by

45 the Yukon River during summer through autumn, Geophys. Res. Lett., 32, 10.1029/2005gl024413, 2005.

Sulzberger, B., and Durisch-Kaiser, E.: Chemical characterization of dissolved organic matter (DOM): A prerequisite for understanding UV-induced changes of DOM absorption properties and bioavailability, Aquat. Sci., 71, 104-126, 10.1007/s00027-008-8082-5, 2009.

Tank, S. E., Fellman, J. B., Hood, E., and Kritzberg, E. S.: Beyond respiration: Controls on lateral carbon fluxes across the terrestrial-aquatic interface, Limnol Oceanogr Lett, 10.1002/lol2.10065, 2018.

50 Vonk, J. E., Tank, S. E., Bowden, W. B., Laurion, I., Vincent, W. F., Alekseychik, P., Amyot, M., Billet, M. F., Canário, J., Cory, R. M., Deshpande, B. N., Helbig, M., Jammet, M., Karlsson, J., Larouche, J., MacMillan, G., Rautio, M., Walter Anthony, K. M., and Wickland, K. P.: Reviews and syntheses: Effects of permafrost thaw on Arctic aquatic ecosystems, Biogeosciences, 12, 7129-7167, 10.5194/bg-12-7129-2015, 2015a.

Vonk, J. E., Tank, S. E., Mann, P. J., Spencer, R. G. M., Treat, C. C., Striegl, R. G., Abbott, B. W., and Wickland, K. P.: Biodegradability

55 of dissolved organic carbon in permafrost soils and aquatic systems: a meta-analysis, Biogeosciences, 12, 6915-6930, 10.5194/bg-12-6915-2015, 2015b.

Walker, S. A., Amon, R. M. W., and Stedmon, C. A.: Variations in high-latitude riverine fluorescent dissolved organic matter: A comparison of large Arctic rivers, J Geophys Res Biogeosci, 118, 1689-1702, 10.1002/2013JG002320, 2013.

Wang, Y., Spencer, R. G. M., Podgorski, D. C., Kellerman, A. M., Rashid, H., Zito, P., Xiao, W., Wei, D., Yang, Y., and Xu, Y.: Spatiotemporal transformation of dissolved organic matter along an alpine stream flow path on the Qinghai–Tibet Plateau: importance of source and permafrost degradation, Biogeosciences, 15, 6637-6648, 10.5194/bg-15-6637-2018, 2018.

Ward, C. P., and Cory, R. M.: Chemical composition of dissolved organic matter draining permafrost soils, Geochim. Cosmochim. Acta, 167, 63-79, 10.1016/j.gca.2015.07.001, 2015.

Ward, C. P., Nalven, S. G., Crump, B. C., Kling, G. W., and Cory, R. M.: Photochemical alteration of organic carbon draining permafrost soils shifts microbial metabolic pathways and stimulates respiration, Nat Commun, 8, 772, 10.1038/s41467-017-00759-2, 2017.

Weishaar, J. L., Aiken, G. R., Bergamaschi, B. A., Fram, M. S., Fujii, R., and Mopper, K.: Evaluation of Specific Ultraviolet Absorbance as an Indicator of the Chemical Composition and Reactivity of Dissolved Organic Carbon, Environ. Sci. Technol., 37, 4702-4708, 10.1021/es030360x, 2003.

Whitehead, R. F., de Mora, S., Demers, S., Gosselin, M., Monfort, P., and Mostajir, B.: Interactions of ultraviolet-B radiation, mixing, and biological activity on photobleaching of natural chromophoric dissolved organic matter: A mesocosm study, Limnol. Oceanogr., 45, 278-291, 10.4319/lo.2000.45.2.0278, 2000.

Woo, M.-K., Kane, D. L., Carey, S. K., and Yang, D.: Progress in permafrost hydrology in the new millennium, Permafr. Periglac. Proc., 19, 237-254, 10.1002/ppp.613, 2008.
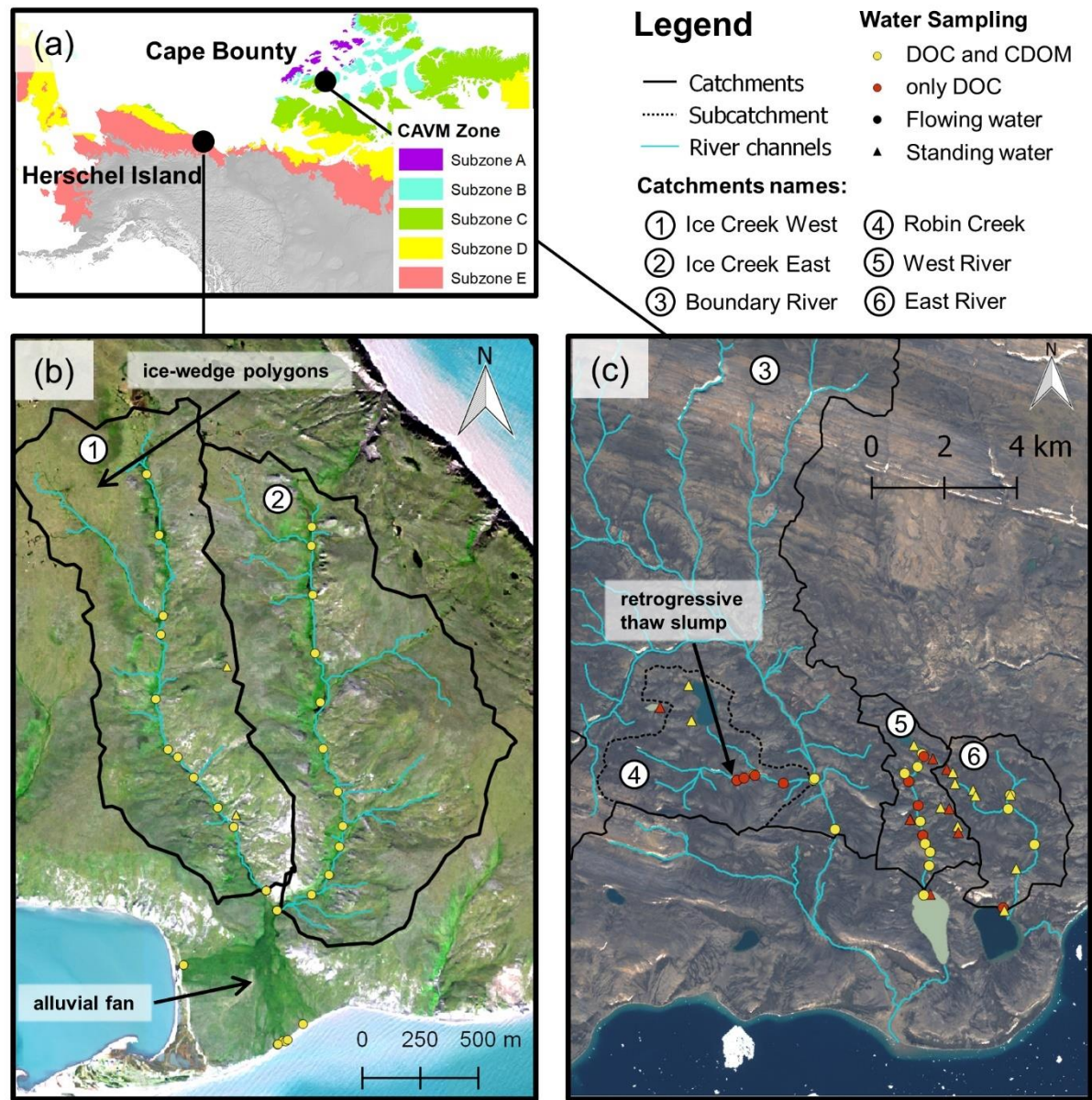
Figures

Figure 1. Maps of the study area showing (a) the location of Herschel Island and Cape Bounty in the Canadian Arctic including the Circumpolar Arctic Vegetation Map (CAVM) bioclimatic zones (Walker & Raymond 2016), (b) the studied catchments Ice Creek West and Ice Creek East on Herschel Island and (c) the studied catchments Boundary River with its subcatchment Robin Creek (dashed watershed), West River and East River. The watershed names are indicated with numbers, and the general flow direction is southwards towards the ocean. Note that samples from flowing water (rivers and streams) are indicated by circles, whereas samples from standing water (ponds and lakes) are indicated by triangles. Yellow colors mark locations where DOC concentration and cDOM measurements are available, while only DOC concentrations are available at red locations. The background images are true color mosaics (Herschel Island: WorldView-3 quasi-true color RGB composite, acquired on 8 August 2015; Cape Bounty: Sentinel-2 quasi-true color RGB composite, acquired on 7 August 2016).
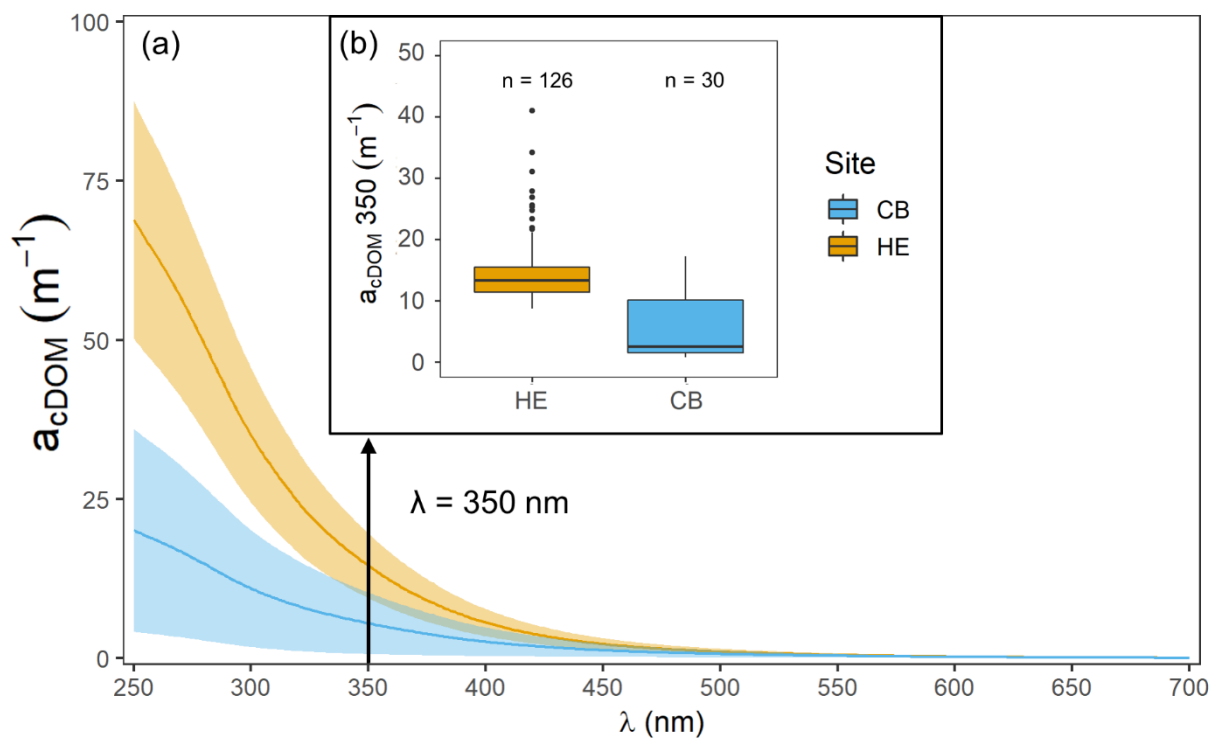
Figure 2. Dissolved organic matter (DOM) absorption characteristics for the sites from Herschel Island (HE, in orange) and Cape Bounty (CB, in blue). (a) Average absorption (m⁻¹) for the wavelengths (λ) between 250 and 700 nm. The colored shaded areas represent the standard deviation from the mean (solid line). (b) boxplots of absorption at 350 nm for both sites.
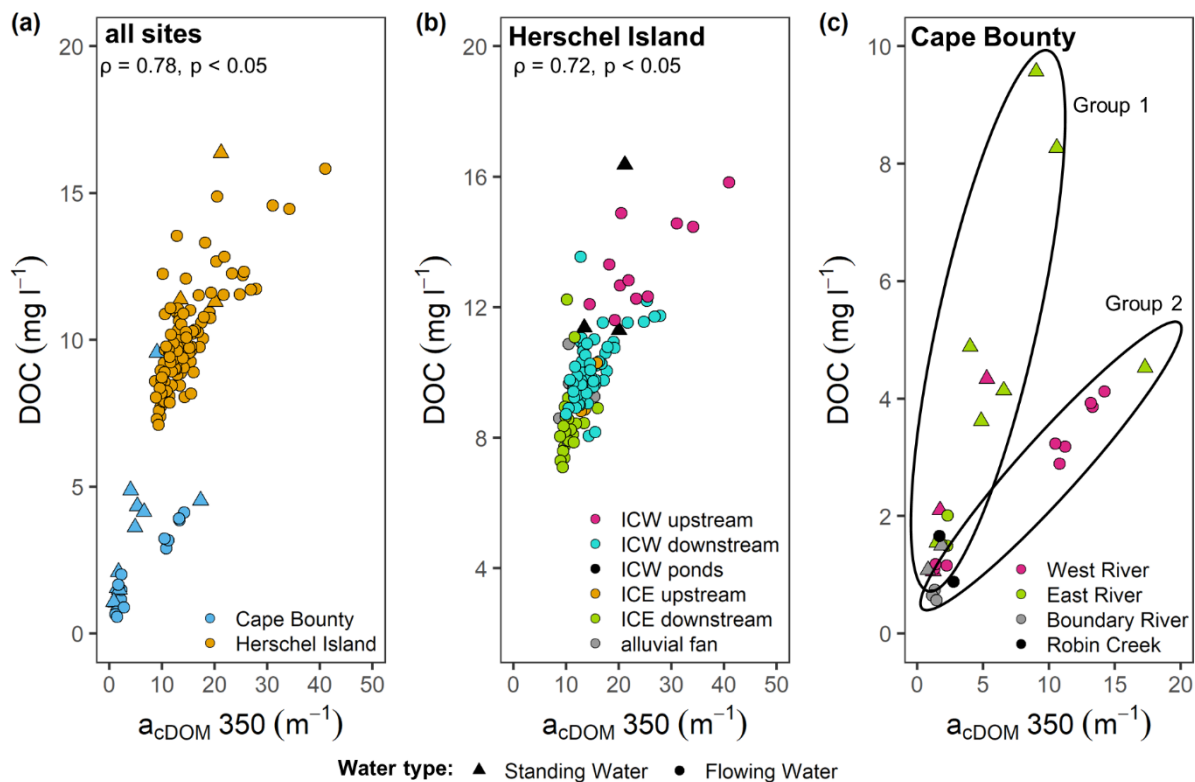
Figure 3. Absorption of colored dissolved organic matter (cDOM) at 350 nm (m[-1]) versus dissolved organic carbon (DOC) concentration (mg l^{-1}) for (a) all sites, (b) sites on Herschel Island depicting the sampling locations Ice Creek West (ICW) upstream, downstream and ponds, Ice Creek East (ICE) upstream and downstream and alluvial fan, and (c) sites at Cape Bounty (West River, East River, Boundary River, Robin Creek). Note that flowing water is indicated by a circle while standing water such as lakes or ponds is indicated by a triangle. The cDOM to DOC relationships are divided in two different groups (c).
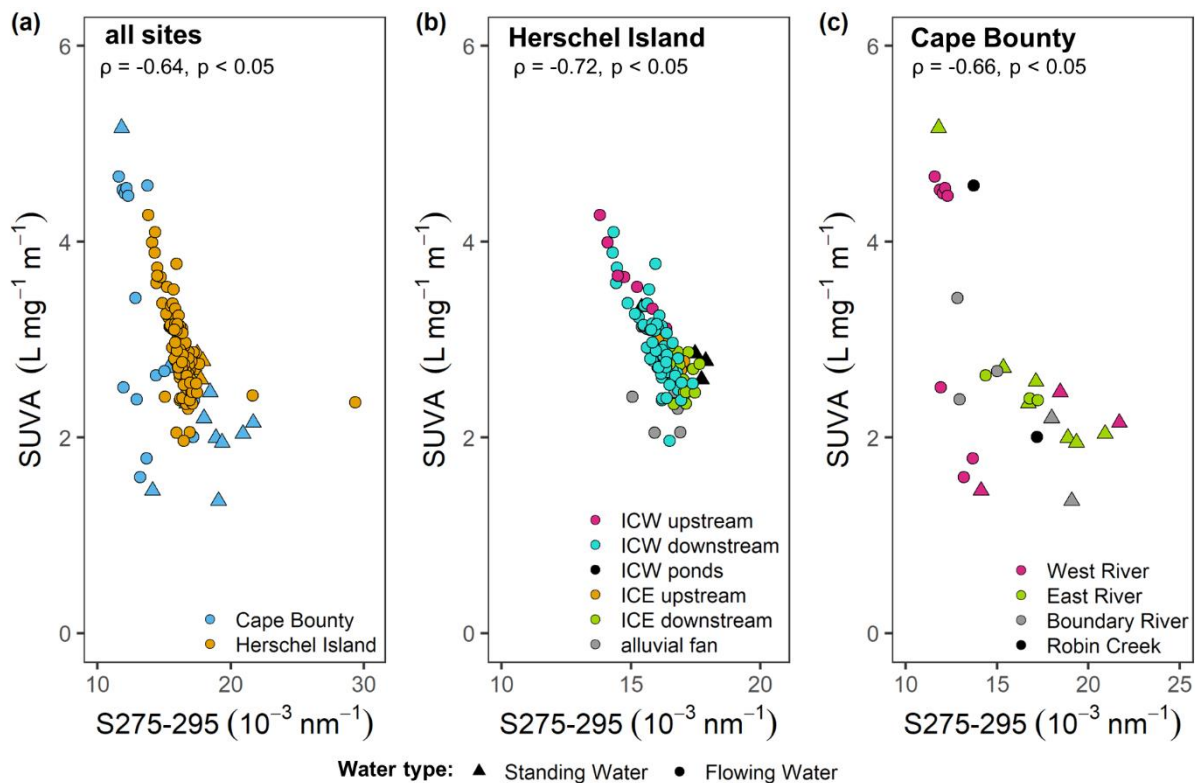
Figure 4. Slope of colored dissolved organic matter ultraviolet cDOM UV absorption 275-295 (10^{-3} nm^{-1}) versus specific ultraviolet absorbance SUVA (L mg^{-1} m^{-1}) for (a) all sites, (b) sites on Herschel Island depicting the sampling locations Ice Creek West (ICW) upstream, downstream and ponds, Ice Creek East (ICE) upstream and downstream and alluvial fan, and (c) sites at Cape Bounty (West River, East River, Boundary River, Robin Creek). Note that flowing water is indicated by a dot while standing water such as lakes or ponds is indicated by a triangle.
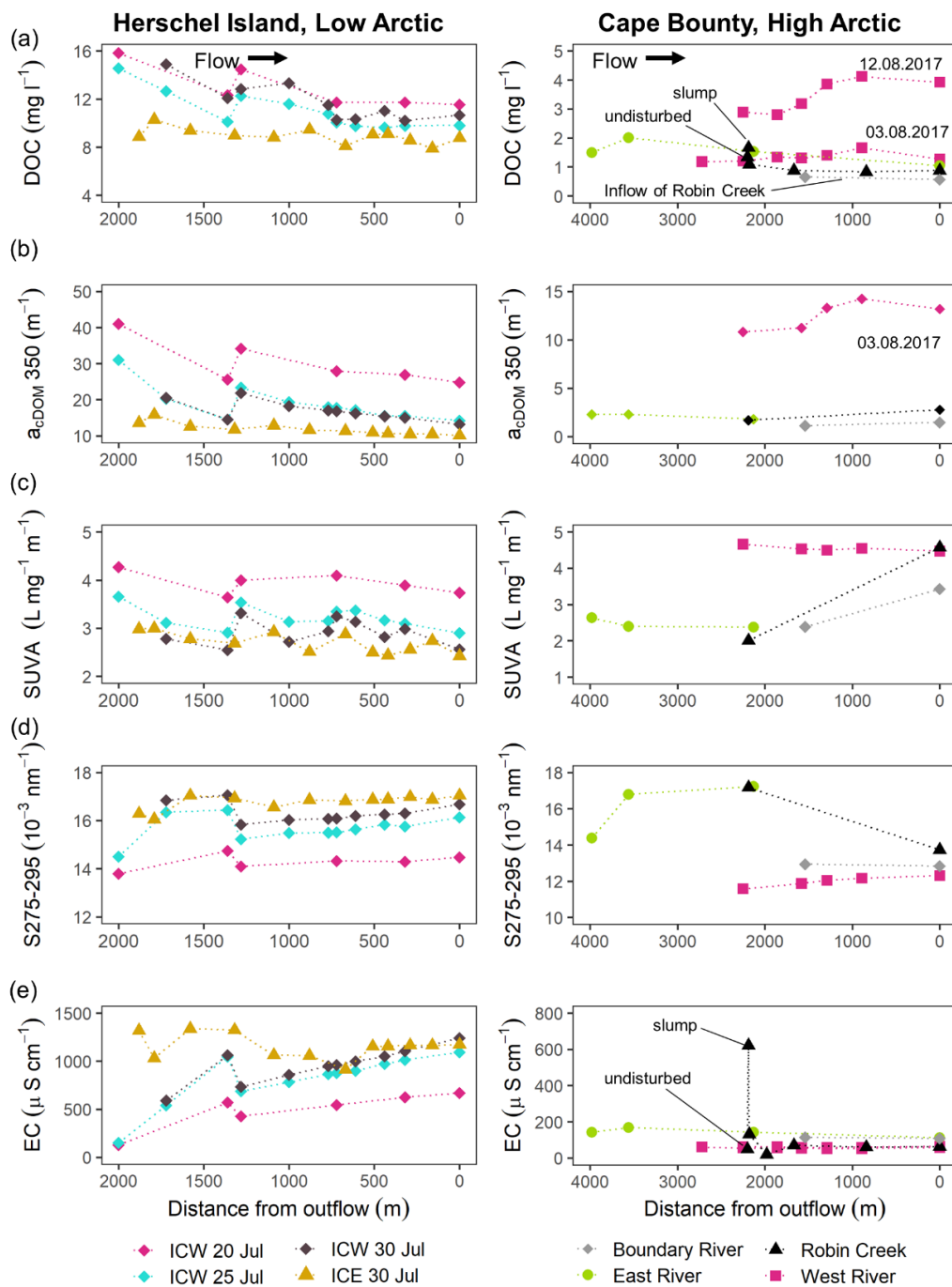
Figure 5. River transects showing values of (a) dissolved organic carbon (DOC) concentration (mg l^{-1}), (b) absorption of colored dissolved organic matter (cDOM) at 350 nm, a$_{cDOM}$350 (m^{-1}), (c) specific ultraviolet absorbance SUVA (L mg^{-1} m^{-1}), (d) cDOM Slope S275-295 (10^{-3} nm^{-1}), (e) electrical conductivity (EC) for rivers on Herschel Island (left) and Cape Bounty (right). Note that Ice Creek West (ICW) and Ice Creek East (ICE) on Herschel Island were sampled at different dates as indicated in the legend.
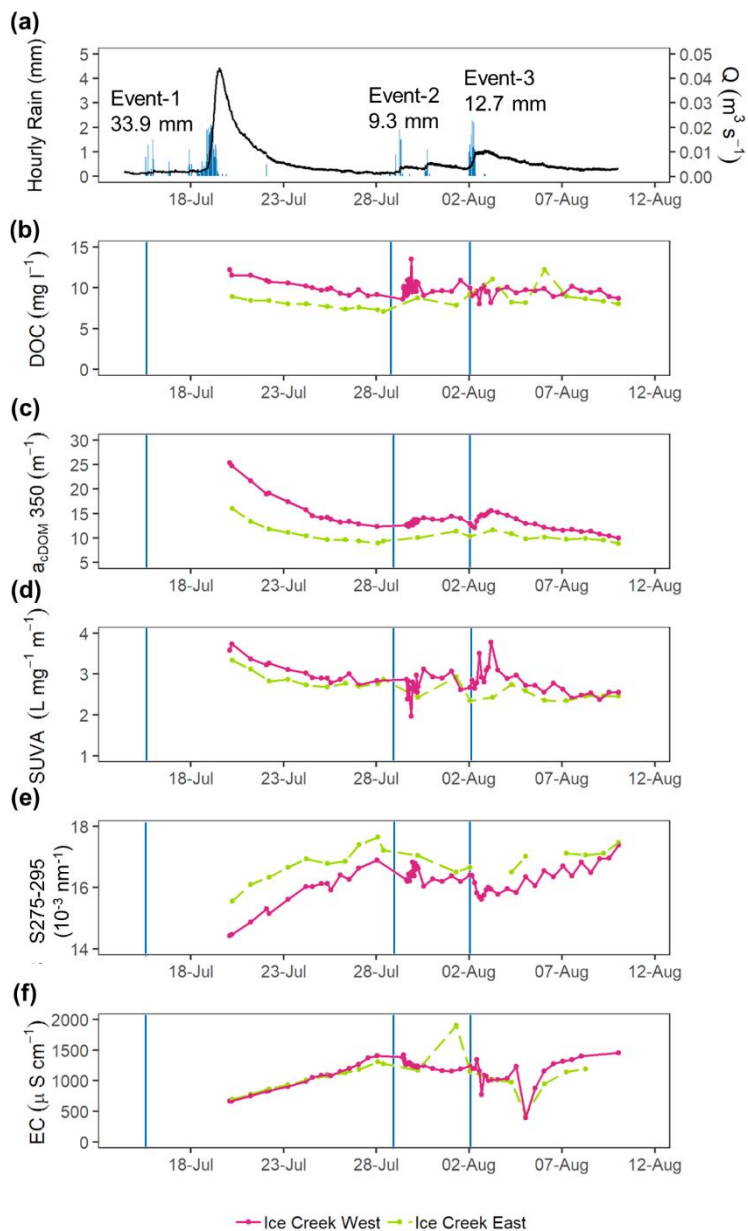
Figure 6. Time series from Herschel Island in 2016 showing (a) Discharge (m^3 s^{-1}) and hourly rainfall (mm) from Ice Creek West, (b) dissolved organic carbon (DOC) concentration (mg l^{-1}), (c) colored dissolved organic matter absorption at 350 nm, a$_{cDOM}$350 (m^{-1}), (d) specific ultraviolet absorbance SUVA (L mg^{-1} m^{-1}) and (e) the cDOM slope S275-295 (10^{-3} nm^{-1}) over the summer season 2016 for Ice Creek West (magenta) and Ice Creek East (green) respectively. The onset of rainfall events is marked with vertical blue lines. As described in the methods, DOC concentrations were corrected between 30 July and 7 August.
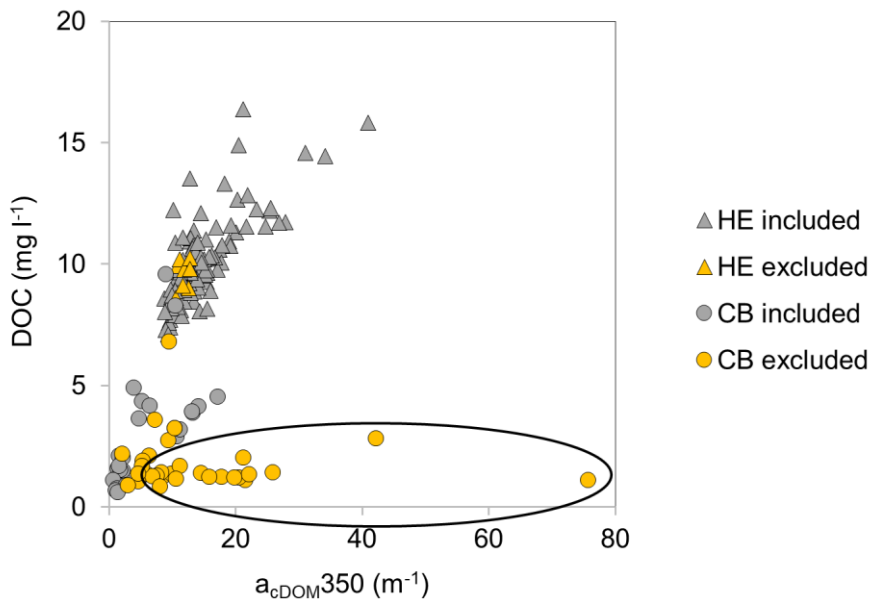
Figure 7. Relationship between colored dissolved organic matter absorption $a_{cDOM}350$ (m^{-1}) and dissolved organic matter concentration DOC (mg l^{-1}) at Herschel Island (HE) displayed as triangle and Cape Bounty (CB) shown as circle. Samples marked in orange were excluded from the study due to flocculation after filtration (section 3.1). The samples circled in black show to high absorption values in relation to the DOC concentration.

Tables

Table 1. Characteristics of studied watersheds on Herschel Island (Low Arctic) and Cape Bounty (High Arctic) showing catchment size (km^2), channel length (km), circumarctic vegetation map (CAVM) bioclimatic zone (CAVM, 2003), soil organic carbon content (SOCC) (Hugelius et al., 2013; Ramage et al., 2019) and maximum catchment elevation above sea level (m).

Site	Catchment size (km^2)	Channel length (km)	Vegetation zone (CAVM)	Soil Organic Carbon content 0-30cm/0-100cm (kg m^2)	Maximum catchment elevation (m above sea level)
Herschel Island, Low Arctic					
Ice Creek West	1.4	2.2	Subzone D	11.4 / 26.4	88
Ice Creek East	1.6	1.9	Subzone D		95
Cape Bounty, High Arctic					
Boundary River	152.5	22.7	Subzone B/C	3.0 / 10.2	213
Robin Creek	14.8	5.1	Subzone B/C		151
West River	8.8	4.2	Subzone B/C		94
East River	12.4	5.2	Subzone B/C		103

5

Table 2. Descriptive statistics (mean ± standard deviation) of dissolved organic carbon, DOC (mg l^{-1}), specific ultraviolet absorbance, SUVA (L mg^{-1} m^{-1}), colored dissolved organic matter absorption at 350 nm, $a_{cDOM}350$ (m^{-1}), cDOM Slope S275-295 (10^{-3} nm^{-1}), slope ratio SR, electrical conductivity EC (µS cm^{-1}), pH and the number (n) of all samples/samples with cDOM absorption measurements. The statistics are given for specific rivers, samples from flowing waters, standing waters and all samples on Herschel Island (HE) and Cape Bounty (CB) respectively. The symbols ">" and "<" indicate significant inter-group differences at the alpha = 0.95 level. When the inter-group differences are significantly different at the alpha = 0.99 level, then they are <u>underlined</u>. When the difference is not significant, "≈" is used.

Site	EC µS cm^{-1}	pH	DOC mg l^{-1}	SUVA L mg^{-1} m^{-1}	$a_{cDOM}350$ m^{-1}	Slope 275-295 10^{-3} nm^{-1}	SR	n
Herschel Island, Low Arctic								
Ice Creek West	1050 ± 310	8.2 ± 0.2	10.4 ± 1.5	3.0 ± 0.4	16.1 ± 5.4	16.0 ± 0.7	0.83 ± 0.02	90/82
Ice Creek East	1030 ± 340	8.2 ± 0.2	8.7 ± 1.1	2.7 ± 0.2	11.1 ± 1.8	17.3 ± 2.4	0.90 ± 0.12	32/32
Alluvial fan	970 ± 170	7.8 ± 0.2	9.2 ± 0.9	2.5 ± 0.4	11.1 ± 1.9	16.3 ± 0.7	0.84 ± 0.02	8/8
Flowing Water (all)	1040 ± 310	8.2 ± 0.2	9.9 ± 1.5	2.9 ± 0.4	14.5 ± 5.1	16.4 ± 1.5	0.85 ± 0.07	130/122
Standing Water (all)	1440 ± 1300	8.3 ± 0.1	12.3 ± 2.8	2.9 ± 0.3	17.0 ± 4.2	17.1 ± 1.2	0.93 ± 0.06	4/4
All samples	1050 ± 370	8.2 ± 0.2	10.0 ± 1.6	2.9 ± 0.4	14.5 ± 5.1	16.4 ± 1.5	0.85 ± 0.07	134/126
Standing (S) vs. Flowing (F)	S ≈ F	S ≈ F	S > F	S ≈ F	S ≈ F	S ≈ F	<u>S > F</u>	n.a.
Cape Bounty, High Arctic								
Boundary River	110 ± 3	7.1 ± 0.0	0.7 ± 0.1	2.8 ± 0.5	1.3 ± 0.2	13.1 ± 1.4	1.13 ± 0.06	3/3
Robin Creek	145 ± 213	7.3 ±0.6	1.1 ± 0.3	3.3 ± 1.8	2.2 ± 0.8	15.1 ± 2.3	1.03 ± 0.12	7/2
West River	60 ± 17	6.9 ± 0.3	2.5 ± 1.7	3.6 ± 1.4	8.5 ± 5.2	11.9 ± 0.8	0.86 ± 0.10	19/8
East River	141 ± 22	7.3 ± 0.1	1.5 ± 0.4	2.5 ± 0.1	2.1 ± 0.3	16.1 ± 1.6	0.95 ± 0.06	4/3
Flowing Water (all)	92 ± 101	7.0 ± 0.4	1.9 ± 1.5	3.2 ± 1.2	5.5 ± 5.1	13.1 ± 2.0	0.94 ± 0.13	33/16
Standing Water (all)	210 ± 160	7.5 ± 0.6	3.4 ± 2.4	2.4 ± 1.0	5.4 ± 4.9	17.4 ± 2.9	1.14 ± 0.20	20/12
All samples	137 ± 136	7.2 ± 0.5	2.5 ± 2.0	2.8 ± 1.1	5.5 ± 4.9	14.8 ± 3.2	1.02 ± 0.19	53/28
Standing (S) vs. Flowing (F)	<u>S > F</u>	<u>S > F</u>	<u>S > F</u>	S < F	S ≈ F	<u>S > F</u>	<u>S > F</u>	n.a.
He_all vs. CB_all	<u>HE > CB</u>	<u>HE > CB</u>	<u>HE > CB</u>	<u>HE > CB</u>	<u>HE > CB</u>	n.a.	<u>HE > CB</u>	n.a.

Table 3. Correlation matrix using the Spearman's rho correlation coefficient between latitude, dissolved organic carbon concentration (DOC), colored dissolved organic carbon absorption at 350 nm (a$_{cDOM}$350), soil organic carbon content (SOCC) in 0-30 cm and 0-100 cm depth (Hugelius et al. 2014). Significance levels of $p < 0.05$ and <u>$p \leq 0.01$</u> are indicated.

	Latitude	a$_{cDOM}$350	DOC	SOCC 0-30cm	SOCC 0-100cm
Latitude	1.00	**<u>-0.22</u>**	**-0.13**	**<u>-0.19</u>**	**<u>-0.26</u>**
a$_{cDOM}$350		1.00	**<u>0.85</u>**	**<u>0.26</u>**	**<u>0.34</u>**
DOC			1.00	**<u>0.53</u>**	**<u>0.51</u>**
SOCC 30cm				1.00	**<u>0.71</u>**
SOCC 100cm					1.00

5